State Space Temporal Gaussian Processes for Glucose Measurements

Ahdab, Mohamad Al; Knudsen, Torben; Leth, John-Josef

Published in:
2022 European Control Conference (ECC)

DOI (link to publication from Publisher):
10.23919/ECC55457.2022.9838040

Publication date:
2022

Document Version
Accepted author manuscript, peer reviewed version

State Space Temporal Gaussian Processes for Glucose Measurements*

Mohamad Al Ahdab[1], Torben Knudsen[1], and John Leth[1]

Abstract— **Measuring the blood glucose (BG) concentrations for people with diabetes is essential to achieve a better glycemic control either by medical professionals or by using feedback control algorithms. Continuous Glucose Monitoring (CGM) devices provide indirect measurements of the BG each 1–5 minutes. However, CGM devices suffer from correlated measurement errors and calibration errors. Detailed models for the errors of CGM devices already exist in the literature. Nonetheless, the identification of these models requires data from multiple CGM devices at once and accurate reference blood glucose measurements obtained clinically. This fact makes these models difficult to be subject-specific during typical treatment since diabetic subjects only use one CGM device with 3–4 finger pricking blood glucose measurements per day. In this paper, a methodology to obtain subject-specific CGM error models using Temporal Gaussian Processes (TGP) in their state space form is introduced. Three different TGPs are proposed and a strategy based on a particle Markov Chain Monte Carlo (MCMC) is used to perform regression and fit parameters for the models. The strategy is tested against data generated from virtual subject using detailed CGM error measurement models which were fitted with more than one CGM device and detailed clinical data from the literature. The results demonstrated the ability for TGP models with the proposed particle MCMC strategy to obtain subject-specific CGM error models using data available during the typical life of diabetic subjects.**

I. Introduction

Subjects with diabetes employ different methods to monitor their BG concentration during their treatment to manage it and to determine appropriate insulin doses. One common method is to use Self-Monitored Glucose Measurement (SMBG) devices which measure glucose concentration in blood drops obtained with a finger prick [1]. Measurements acquired from such devices are sparse and do not provide enough information about the variability of glucose concentration. On the other hand, CGM devices provide measurement samples each 1-5 minuts allowing for a better description of glucose variability. Obtaining a better description about glucose variability with CGM devices has been shown to provide improvement in glycemic control and detection of low BG concentrations [2]. Nevertheless, CGM devices do not provide direct measurement of BG. Instead, CGM devices measure the interstitium glucose (IG) concentration, and therefore, there is a time lag between CGM measurements and BG concentrations which depends on the diffusion process of BG to IG. Additionally, CGM devices have been shown to be affected by systematic and random errors [3]. Therefore, patients usually use SMBG measurement to calibrate CGM devices during the day [4]. Obtaining and fitting subject-specific models for the errors of CGM devices is important for more accurate automated insulin dose calculators and fitting personalised insulin-glucose dynamical models for patients [5], [6].

In the literature, several models exist for the error of CGM measurements with various degrees of complexity. In [7], a posteriori recalibration of CGM is performed first using BG references with a sample time of 15 minutes for around 40 hours. After that, a first order model between BG and IG is used with a fixed time constant of 17 minuts to estimate IG based on interpolated reference BG data. Finally, the residual between CGM and the estimated IG, taken as the measurement noise of the sensor, is fitted with a first order autoregressive (AR) model. The work in [8] then refined the work in [7] by considering forcing functions. Values for the time constant for the BG to IG kinetics were also estimated for each individual subject with the help of BG reference values collected every 15 minutes through BG a venous cannula. The work in [9]–[12] considered a more detailed model with reference BG sampled more frequently and multiple CGM devices. The models consider polynomials in time for both the gain and the drift on the CGM measurements in addition to modeling the additive random error as the sum of two different second order AR processes AR(2). Lastly, AR(2) models for both the drift and the additive noise are used to model continuous intravascular glucose monitoring sensor. Each of the mentioned methods above relied on reference BG values taken more frequently than the usual case of SMBG measurements. This make these models difficult to be used in subject-specific settings. The works in [13]–[15] intended to improve CGM measurements with the help of Kalman filters using the typical SMBG data patients provide. In [13], an extended Kalman filter (EKF) is used to estimate BG concentrations from SMBG and CGM measurements. The model for the EKF consists of a first order model with a time constant assumed between IG and BG, a random walk model for BG and other constant parameters to be estimated, and an additive Gaussian noise for the measurements of SMBG and CGM with the latter having a scale parameter on IG that was estimated. The variance of the additive noise on SMBG was assumed to be proportional to percentage of the SMBG value while the variance for CGM measurememnts was fixed to constant value and was not estimated. In [14], a dual rate Kalmanfilter is used on a similar model to the one in [13] but now the rate of change for BG and the scale parameters evolve to two independent random walks. Additionally, no model for IG to BG concentrations is assumed. Moreover,

*This work was funded by the IFD Grand Solution project ADAPT- T2D, project number 9068-00056B.

[1]The authors are with Section of Automation and Control, Department of Electronic Systems, Aalborg University, Aalborg Øst, Denmark {maah, hgcl, tk, jjl}@es.aau.dk

the variance on SMBG was also assumed to be constant and known. Finally in [15], an EKF is used similarly to the one in [13] but with the assumption that the scale parameters evolves according to a triply integrated white noise while the BG evolves according to a doubly integrated white noise. Additionally, the time constant parameter was not estimated between IG and BG due to the difficulties in estimating it with sparse SMBG measurements. Nevertheless, the proposed EKF strategy was shown to be robust to the different values of the time constant. As for the variances, only the variance of the white noise associated with the scale parameters was estimated. The rest of the variances were fixed to be the same variances used in simulation. All the mentioned methods did not attempt to estimate variances for measurement noises. Moreover, they all assumed an additive gaussian noise for CGM measurements. Additionally, all the of these methods assumed integrated white noise models for the evolution of BG. Their main intention was to improve the CGM measurements rather than obtaining a subject-specific CGM model.

As for SMBG models, several models have been concerned through the literature with various degrees of complexity. Some works, such as [16], [17], assumed that the relative error of the SMBG measurement to be an identically and independently distributed (iid) Gaussian process with a bias term. Others, as in [18], modelled the error on SMBG measurement to be gaussinally distributed with zero mean and variances depending on the BG concentration. More specifically, the variance of the error was assumed constant for BG below 4.2 $[\mathrm{mmol/L}]$ and linearly dependent on BG for BG above 4.2 $[\mathrm{mmol/L}]$. This assumption was done to simulate the International Organization for Standardization (ISO) standard for SMBG devices [19]. The ISO standard states that 95 percent of glucose measurement should lie within ± 0.83 $[\mathrm{mmol/L}]$ when BG concentration is below 4.2 $[\mathrm{mmol/L}]$ and within 20% of BG values when BG concentration is above 4.2 $[\mathrm{mmol/L}]$. Recently, [11] considered two different skew normal distributions for the SMBG relative error when BG concentrations are above 4.2 $[\mathrm{mmol/L}]$ and the SMBG error when BG concentrations are below 4.2 $[\mathrm{mmol/L}]$. Parameters for the two different distribution were estimated in addition to parameters for exponential distributions accounting for outliear measurements. To be able to estimate the parameters of the error distributions, highly accurate reference BG data obtained by a laboratory equipment each 15 minutes in parallel to SMBG measurements were used. The main contribution of this paper is as follows. We propose a new strategy based on TGP to obtain subject-specific CGM error models using SMBG and CGM measurements. Additionally, we propose to model the CGM errors with only one CGM device and SMBG measurements unlike the other strategies which uses multiple CGM devices and/or reference BG samples obtained with a relatively higher sampling rate than SMBG measurements. The structure of the paper is as follows. Section III presents an introduction to TGP regression. After that, we present the proposed models for the CGM and SMBG errors in section IV. The regression strategy is then presented in section V. Subsequently, we present simulation models in section VI to generate data and compare with our proposed strategy to later be followed with results in section VII and a conclusion in section VIII.

II. NOTATIONS

All probabilistic considerations in this paper will be with respect to an underlying probability space $(\Omega, \mathcal{F}, \mathbb{P})$. For a random variable x we write $\mathsf{x} = x(\omega)$ for the value of the random variable, and $x \sim p(\mathsf{x})$ for the corresponding density. We use $\mathcal{N}(\mu, \sigma)$ to denote the normal distribution with mean μ and variance σ. If the difference between two consecutive time instants t_k and t_{k+j} is such that $t_{k+j} - t_k = jT,\ j \in \mathbb{Z}$ with $T \in \mathbb{R}$ being a constant, then variables that are indexed with time $x(t_k), x(t_{k+j})$ will be denoted by $x(k), x(k+j)$ for ease of notations. For a collection of $n \in \mathbb{Z}$ variables $\{x(i)\}_{i=1}^{n}$ or $\{x(t_i)\}_{i=1}^{n}$, the notation $x^{1:n}$ is used for both of them. Moreover, if each of $\{x(i)\}_{i=1}^{n}$ is a scalar, then $x^{1:n} = \big[x(1), \ldots, x(n)\big]^{\mathrm{T}}$. In addition, for a diagonal matrix $A_{n\times n}$ with diagonal elements $a_1, \ldots, a_n$, the notation $A = \mathrm{diag}\,(a_1, \ldots, a_n)$ is used. Moreover, the symbol I_n is used to denote an n dimensional identity matrix and the symbol $\mathbf{1}_n$ is used to denote an n dimensional column vector of 1s.

III. GAUSSIAN PROCESS REGRESSION

A TGP is a stochastic process $f(t)$ indexed by time inputs $t \in \mathbb{R}_{\geq 0}$ such that any finite collection of the random variables $\{f(t_1), \ldots, f(t_n)\}$ has an n-dimensional Gaussian distribution [20]. The TGP regression address the estimation of the statistics of $f(t^*)$ with t^* being an arbitrary point in time given a set of data $\{t_i, \mathsf{y}(t_i)\}_{i=1}^{n}$ with output $\mathsf{y}(t_i)$ being the value $\mathsf{f}(t_i)$ corrupted with noise e.g.,

$$y(t_i) = f(t_i) + \varepsilon_i \tag{1}$$

with $\varepsilon_i \sim \mathcal{N}(\mu_{\epsilon_i}, \sigma_{\epsilon_i})$.

The TGP regression uses the fact that the joint distribution of any finite collection of its random variable is Guassian, and therefore completely determined by its mean and covariance functions. A TGP process is commonly denoted as

$$f(t) \sim \mathcal{GP}\left(\mu(t), \mathrm{c}\left(t, t^{'}, \theta_{\mathrm{c}}\right)\right) \tag{2}$$

with $\mu(t)$ the mean function and $\mathrm{c}\left(t, t^{'}, \theta_{\mathrm{c}}\right)$ the covariance function between time points t and $t^{'}$ with hyperparameters θ_{c}. The the mean and the covariance functions represent part of the prior information regarding the process. For this paper, we assume that $\mu(t) = 0$ and restrict the prior information in the choice of the TGP model to be provided by $\mathrm{c}\left(t, t^{'}, \theta_{\mathrm{c}}\right)$ as a first approach towards using TGP for CGM error models. Given the collection $\{t_i\}_{i=1}^{n}$, one can write as a prior $f(t_1), \ldots, f(t_n) \sim \mathcal{N}\,(0, \mathrm{C})$ where the ijth entry of the covariance matrix C is $\mathrm{C}_{ij} = \mathrm{c}\left(t_i, t_j, \theta_{\mathrm{c}}\right)$.

The computational complexity for TGP can scale up to $\mathcal{O}(n^3)$ for all kinds of output processes, even in the Gaussian case (1), see [20]. This can be a problem for large data sets.

Especially when time is the input and the sampling frequency is high as it is the case for CGM measurements. One way to deal with this is to use state space representation for TGPs. In [21], [22], exact or approximate methods to obtain state space representations for TGPs with stationary covariance function ($\mathrm{c}(t, t^{'}, \theta_{\mathrm{c}}) = \mathrm{c}(\tau, \theta_{\mathrm{c}}),\ \tau = t - t^{'}$) have been presented and discussed. In addition, the regression problem for TGPs in (2) with a general likelihood can be seen as a smoothing problem for the likelihood together with the following linear system

$$\mathrm{d}x_{gp}(t) = A_{gp}x_{gp}(t)\mathrm{d}t + L_{gp}\mathrm{d}B \tag{3a}$$

$$f(t) = H_{gp}x_{gp}(t) \tag{3b}$$

with B denoting standard Brownian motion. The stationary covariance functions determines the matrices A_{gp}, L_{gp}, and H_{gp} together with the state dimension. For some covariance functions, exact state representation can be found in closed form as shown in [21], [22]. For example, the TGP with an exponential covariance function is represented by an Ornstein–Uhlenbeck (OU) process.[1]Other example which have closed form state space representation are TGPs with half integers Matérn covariance functions. For other stationary covariance functions such as the squared exponential function, they can be approximated using Taylor series or Padé approximation for their spectral density to obtain an approximate linear state representation as done in [21], [23].

IV. Regression Model

A. CGM model

To consider that CGM devices measure IG instead of BG, a first order model is considered between the two concentration with time constant τ_c $[\mathrm{min}^{-1}]$ as done in [9], [15]

$$\mathrm{d}x_c(t) = \frac{1}{\tau_c}\left(x_g(t) - x_c(t)\right)\mathrm{d}t \tag{4}$$

with x_g $[\mathrm{mmol/L}]$ the BG concentration, and x_c $[\mathrm{mmol/L}]$ is the IG concentration. The time constant τ_c is taken to be the median from [9] which is 7 $[\mathrm{min}^{-1}]$. For the CGM measurement, the model is assumed in this paper to be on the form

$$y_c(k) = \left(1 + g(k)\right)x_c(k) + v(k) + \varepsilon_c(k),\ \varepsilon_c(k) \sim \mathcal{N}(0, \sigma_c^2), \tag{5}$$

where $t_{k+j} - t_k = jT_s, j \in \mathbb{Z}$ with T_s being the sampling time of the CGM device. The process $g(k)$ represents the time dependent gain error of the sensor due to calibration. As for $v(k)$ and $\varepsilon_c(k)$, they represent the additive calibration and measurement errors of the sensor. In this paper, three different models are assumed for $g(k)$ and $v(k)$ summarized in Table I. For the first model, the additive noise is assumed to be an AR(2) process, inspired by [9]. As for the gain error, the exponential covariance function (OU) is chosen inspired by the work in [14] since their model for the gain error can assumed to be a discritized version of an OU process. Additionally, the induced OU model is simple since it becomes one dimensional. Nevertheless, the solutions for the OU process are continuous but not differentiable which is not an ideal property for the gain error. For the second model, a TGP with a squared exponential covariance function is considered instead of an AR(2) process. The squared exponential covariance function gives solutions which are infinitely differentiable. Moreover, it is a common choice for covariance functions in TGPs when no information about the underlying true process is known [20]. However, the squared exponential kernel cannot be exactly represented by a finite linear system in the form of (3). Instead, a 6th order Taylor series approximation for the spectral density of the covariance function is used in this paper to obtain a 6th order state space representation [22], [23]. Finally, the third model considers two different TGPs with a Matérn 5/2 covariance functions. The Matérn 5/2 covariance functions can be written as the product of a second degree polynomial and an exponential covariance function. This choice was made here since the works in [9]–[12], [24] all considered polynomials in time for the sensor's calibration error with a maximum degree of two. Additionally, TGPs with the Matérn 5/2 covariance function have an exact third order state space representation [21], [22].

Model Number	$g(k)$	$v(k)$
Model 1	Exponential (OU)	AR(2)
Model 2	Exponential (OU)	Squared Exponential
Model 3	Matérn 5/2	Matérn 5/2

TABLE I
Different models of CGM considered in the paper

The aim of this paper is to provide a methodology for the use of TGPs with CGM and SMBG measurements, and to demonstrate the ability of TGPs to model CGM measurements with only one CGM device and SMBG measurements.

To avoid a model for the BG concentration x_g, the dynamics in (4) is discretized using forward Euler discritization with the sampling time T_s to obtain

$$x_c(k+1) = (1 - \frac{T_s}{\tau_c})x_c(k) + \frac{T_s}{\tau_c}x_g(k). \tag{6}$$

Now, $x_g(k)$ can be written in terms of $y_c(k+1)$ and $y_c(k)$ by isolating $x_g(k)$ in (6) and using (5) to obtain

$$\begin{aligned} x_g(k) = \frac{\tau_c}{T_s}\frac{y_c(k+1) - v(k+1) - \varepsilon_c(k+1)}{1 + g(k+1)} \\ - \left(\frac{\tau_c}{T_s} - 1\right)\frac{y_c(k) - v(k) - \varepsilon_c(k)}{1 + g(k)}. \end{aligned} \tag{7}$$

B. SMBG

The SMBG measurements are modelled as

$$y_s(t_s) = x_g(t_s) + \sigma_s\left(x_g(t_s)\right)\varepsilon_s(t_s), \tag{8a}$$

$$\sigma_s\left(x_g\right) = \frac{1}{\kappa}\sigma_2 \log\left(1 + \mathrm{e}^{\kappa\left(x_g - 4.2\right)}\right) + \sigma_1, \tag{8b}$$

where t_s is the time instant of the measurement. The model for the standard deviation (8b) is chosen such that it provides a smooth transition between the two zones (mentioned in the

[1]For a scalar OU TGP with $c(t, t^{'}) = \frac{\sigma^2}{2\gamma}\mathrm{e}^{-\gamma|t - t^{'}|}$, $A_{gp} = -\gamma,\ L_{gp} = \sigma^2,\ H_{gp} = 1$

introduction) which simulates the ISO standard for SMBG devices [19]. The value of κ determines how smooth the transition is. For this paper, a value of $\kappa = 5$ is chosen to produce the function in Figure 1.

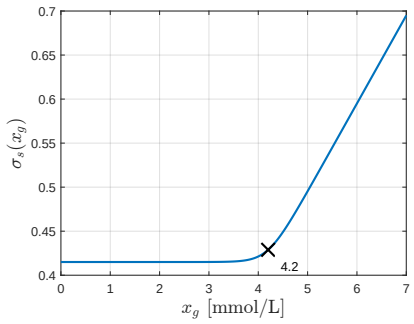

Fig. 1. A plot of $\sigma_s\left(x_g\right)$ for $\kappa = 5$. The values of σ_1 and σ_2 are chosen in accordance to the ISO [19] to be $\sigma_1 = 0.415$ [mmol/L] and $\sigma_2 = 0.1$.

Note that it is now possible to write the measurement models here in a state space representation where the dynamics are given by the state space representation of $g(k)$ and $v(k)$ (discrtized in case of a TGP using Euler–Maruyama), and the output equation is (8) with $x_g(k)$ given by (7). This can be done by matching SMBG measurements at time t_s with the nearest CGM measurement t_k. For the following sections, $x_g(k) \in \mathbb{R}^{n_g}, x_v(k) \in \mathbb{R}^{n_v}$ are denoted for the states corresponding to the model of $g(k), v(k)$ respectively, and $x(k) = [x_g^{\mathrm{T}}(k), x_v^{\mathrm{T}}(k)]^{\mathrm{T}}$. The overall state space model can then be written in the following form

$$x(k+1) = Ax(k) + L\zeta(k),\ \zeta(k) \sim \mathcal{N}(0, \sqrt{T_s}\mathrm{I}_{n_g+n_v}), \tag{9a}$$

$$\begin{bmatrix} g(k) \\ v(k) \end{bmatrix} = Hx(k). \tag{9b}$$

with the output equation given by (7) and (8), and

$$A = \begin{bmatrix} (\mathrm{I}_{n_g} + T_s A_g) & 0 \\ 0 & (\mathrm{I}_{n_v} + T_s A_v) \end{bmatrix}, \tag{10a}$$

$$L = \begin{bmatrix} L_g & 0 \\ 0 & L_v \end{bmatrix}, \tag{10b}$$

$$H = \begin{bmatrix} H_g & 0 \\ 0 & H_v \end{bmatrix}, \tag{10c}$$

with A_g, L_g, H_g and A_v, L_v, H_v the corresponding state space matrices for $g(k)$ and $v(k)$ respectively.

V. Regression Strategy

As discussed in [22], regression of TGPs can be done using smoothing techniques when they are represented as a state space model. The two TGPs considered in this paper come together in a nonlinear fashion as in (7). Additionally, the noise for the likelihood in (8) is clearly not additive Gaussian noise. Moreover, the SMBG measuremens which are the outputs of the modeling strategy proposed in section IV happens only 3-4 times per day. Due to these reasons, a particle smoother is considered for the regression of the model. In addition to the smoothing, it is desired that the strategy should also estimate the hyper parameters of the TGP covariance functions (or the AR(2) process) θ_g and θ_v of $g(k)$ and $v(k)$ respectively. In addition, the strategy is also desired to estimate σ_1 and σ_2 in (8b), and σ_c in (5) to have $\theta = \begin{bmatrix} \theta_g^{\mathrm{T}} & \theta_v^{\mathrm{T}} & \sigma_c & \sigma_1 & \sigma_2 \end{bmatrix}^{\mathrm{T}}$ as the overall parameters desired to be estimated. For these reasons, Particle Gibbs with Ancestor Sampling (PGAS) [25] together with Metropolis Hasting (MH) [26] are chosen as a smoothing (regression) and a parameter estimation strategy. PGAS is a particle MCMC algorithm which combines Sequential Monte Carlo methods with MCMC. MCMC strategies are concerned with obtaining samples from a desired density by means of sampling a Markov chain from a transition kernel which has the desired density as its unique stationary density. Thus, from an arbitrary initial state of the Markov chain, successive samples (by the ergodicity property of the Markov kernel) from the transition kernel will approximate samples from the target density, provided that the Markov chain has reached its stationary distribution. The PGAS is constructed as an ergodic kernel with the stationary density being the smoothing density $p(\mathsf{x}^{1:N}|\mathsf{y}_s^{1:N_s}, \theta)$, where N is the number of CGM samples and N_s is the number of SMBG measurements matched with the CGM measurements. Thus, one can use the PGAS to obtain M subsequent samples $\mathsf{x}^{1:N}[1], \ldots, \mathsf{x}^{1:N}[m], \ldots, \mathsf{x}^{1:N}[M]$ approximately from the smoothing distribution by running the kernel with $\mathsf{x}^{1:N}[m-1]$ to obtain $\mathsf{x}^{1:N}[m]$. Additionally, if it is desired to estimate parameters, then one can use the PGAS kernel in another MCMC sampling procedure such as Gibbs sampling [27] in order to sample parameters from their posterior density as shown in Algorithm 1. For the model in this paper, it is possible to know the posterior up to a proportionality constant

$$\log\left(p\left(\theta|\mathsf{x}^{1:N}[m], \mathsf{y}_s^{1:N_s}\right)\right) = -\frac{1}{2}\sum_{i=1}^{N_s}\log\left(2\pi\sigma_s^2\left(\mathsf{x}_g(i)\right)\right)$$

$$-\frac{1}{2}\sum_{i=1}^{N_s}\frac{\mathsf{y}_s(i) - \mathsf{x}_g(i)}{\sigma_s^2\left(\mathsf{x}_g(i)\right)} + \log(p(\theta)) + \text{constant},$$

Note that $\mathsf{x}_g(i)$ depends on the parameters θ and $\mathsf{x}^{1:i+1}[m]$, despite this not being indicated in the notation. To sample from the posterior distribution, another MCMC algorithm can be used. In this paper we used the MH to sample from the posterior $p\left(\theta|\mathsf{x}^{1:N}[m], \mathsf{y}_s^{1:N_s}\right)$. The proposal density of the MH algorithm is chosen to be a random walk driven by white noise for all the parameters. Note that the complexity order of the PGAS in [25] is $\mathcal{O}\left(NN_p\right)$ and $\mathcal{O}\left(NN_pM\right)$ for smoothing with N_p being the number of particles. For the PGAS, it was shown that it still provides good mixing for low number of particles due to the ancestor sampling step introduced in [25], even for $N_p = 5$ particles.

VI. Simulation Model

A. Generating Virtual Diabetic subjects Data

The model from [28] is used to generate IG and BG data of 100 type 2 diabetic subjects for 10 days. The BG concentration is taken to be the glucose concentration in

Algorithm 1: Gibbs sampling with PGAS

Input: Arbitrary $\mathsf{x}^{1:N}[1]$ and $\theta[1]$, a prior distribution for the parameters $\theta \sim p(\theta)$, and N_s measurements $\mathsf{y}_s^{1:N_s}$

Output: A sequence of samples $\mathsf{x}^{1:N}[1], \ldots, \mathsf{x}^{1:N}[M]$ and $\theta[1], \ldots, \theta[M]$

For $m = 2, \ldots, M$ **Do**

Run the PGAS kernel with $\mathsf{x}^{1:N}[m-1]$ to obtain $\mathsf{x}^{1:N}[m]$ given $\theta[m-1]$ see [25].

Sample $\theta[m]$ from the posterior $p\left(\theta|\mathsf{x}^{1:N}[m], \mathsf{y}_s^{1:N_s}\right)$.

End For

the heart and lung compartment, while the IG concentration is taken to be the glucose concentration in the periphery interstitial fluid compartment. To simulate different subjects, specific parameters from the model are changed randomly from subject to subject according to [29]. Moreover, the time constant to the periphery interstitial fluid compartment is changed uniformly for each subject within an interval of 40% of its nominal value to simulate the effect of different time lags between IG and BG. Additionally, subjects consume three different meals per day denoted as breakfast, lunch, and dinner. The meals are allocated randomly within the following time intervals: 6:00-8:00 [h] for breakfast, 12:00-14:00 [h] for lunch, and 19:00-21:00 [h] for dinner. The Carbohydrate intake for each meals is also drawn randomly from a normal distribution with mean $\pm$ SD given by 45 ± 10 [g] for breakfast, 75 ± 10 [g] for lunch, and 85 ± 10 [g] for dinner. The simulated subjects took 4 SMBG measurements. One measurement time drawn uniformly 10–30 [min] before breakfast, one drawn uniformly 30–90 [min] after breakfast, another drawn uniformly between 10–30 [min] before dinner, and one drawn uniformly 30-90 [min] after dinner. This scheduling is usually done by subjects since they likely measure their BG concentration before a meal to determine how much they can eat and later after the meal to check their BG after meal consumption. In addition to the 4 SMBG measurements, a measurement is taken by the subject whenever BG goes below 4 [mmol/L]. This is also usually done since subject can feel low BG episodes and would likely take an SMBG measurement to check it. Finally, all subjects are assumed to take constant long acting insulin doses each day starting from 30 units of insulin and increasing by 10 units for each three days. This choice was done to insure that some of the subject will have low BG episodes.

B. Generating CGM and SMBG Measurements

To generate CGM data for the generated IG data, the polynomial and AR(2) models discussed in [9]–[12], [24] are used. Each of the references used polynomials for the calibration gain error and for the calibration additive error with different degrees and piece-wise constant coefficient between calibration points. The degrees of these polynomial differed from article to article depending on the device used in the study, the data set used, and the day in which the identification is carried out ([10] identified polynomials with different degrees for Day 1, Day 4, and Day 7 of the CGM device). Additionally, two additive random errors are modeled with two separate AR(2) process. The first random error represent random calibration error, and the second one represent other random measurement errors. In order to simulate these models with polynomials of different degrees, a count for how many times an n_{pg}th and an n_{pv}th degree polynomial is used for the calibration gain error and the calibration additive error respectively has been done. Afterwards, for each subject, the degrees of the polynomials associated with their CGM measurements is drawn randomly according to the following categorical (multinoulli) distribution obtained by the counts of the polynomials For the

	$n_{pg}=0$	$n_{pg}=1$	$n_{pg}=2$
$n_{pv}=0$	4/15	2/15	×
$n_{pv}=1$	2/15	5/15	1/15
$n_{pv}=2$	×	1/15	×

TABLE II

PROBABILITIES FOR THE POLYNOMIAL DEGREE USED TO SIMULATE CGM DEVICES. THE × IS USED FOR CASES WHICH WERE NOT REPORTED IN THE LITERATURE AND THUS HAS NO PROBABILITY

coefficients of the calibration gain error polynomial $\alpha = [\alpha_0\ \alpha_1\ \alpha_2]^{\mathrm{T}}$ and the coefficients of calibration additive error polynomial $\beta = [\beta_0\ \beta_1\ \beta_2]^{\mathrm{T}}$, a normal distribution is fitted for the coefficients $\alpha \sim \mathcal{N}(\mu_\alpha \Sigma_\alpha)$, and $\beta \sim \mathcal{N}(\mu_\beta, \Sigma_\beta)$ based on a collection of the coefficient's statistics provided in the references [9]–[12], [24] with

$$\mu_\alpha = \begin{bmatrix} 1.001 & 2.066 \times 10^{-5} & 0 \end{bmatrix}^{\mathrm{T}}, \tag{11a}$$

$$\Sigma_\alpha = \mathrm{diag}\begin{pmatrix} 0.0625 & 7.225 \times 10^{-5} & 1.936 \times 10^{-5} \end{pmatrix}, \tag{11b}$$

$$\mu_\beta = \begin{bmatrix} -0.0175 & 0.002 & 4.480 \times 10^{-5} \end{bmatrix}^{\mathrm{T}}, \tag{11c}$$

$$\Sigma_\beta = \mathrm{diag}\begin{pmatrix} 4.297 & 5.138 \times 10^{-7} & 2.009 \times 10^{-9} \end{pmatrix}. \tag{11d}$$

Moreover, a negative cross correlation term of -0.95 between the coefficients for the calibration gain error polynomials and the coefficients for the calibration additive error polynomials is added according to the reported results by [9]. Finally, the coefficient for the two AR(2) process are taken from the population reported in [10]. Simulating CGM errors with this approach produces a wide variety of cases to test against due to the way the parameters are sampled. This is in line with the aim of this paper which is to test the validity of using GP models as CGM error models derived with one CGM device and SMBG measurements. Note that this simulation approach can generate improbable cases. However it does not invalidate the method used in this paper, quite the contrary, it demonstrates the robustness of the method. For the SMBG measurements, the two zones skew normal distributions for One Touch Ultra 2 (OTU2) device is used [11].

VII. Results and Discussion

Each of the 100 patients' CGM and SMBG, generated as described in section VI, were used in Algorithm 1 with the three proposed different models in Table I. The prior for each parameter was chosen to be uniform between 0 and 10 since all of them are positives. The algorithm was used to generate $M = 10000$ Markov chain samples of $x^{1:N}$ and θ. For sample $\mathsf{x}^{1:N}[m]$ of the Markov chain, 300 samples of parameters are drawn using the MH strategy and only the last sample is taken to be $\theta[m]$. This is done to try to ensure that the Markov chain sample of the MH strategy is an approximate sample from the posterior in (V). For the PGAS, the number of particles is chosen to be 20. To ensure that the samples of trajectory and parameters are from the smoothing and posterior distribution respectively, the last 1000 of the Markov chain sample are considered.

To asses the smoothing and modeling strategy in this paper, the last 1000 smoothed samples $\{\mathsf{x}^{1:N}[m]\}_{m=M-1000}^{M}$ are used to generate estimates of $\{\hat{\mathsf{x}}_g^{1:N}[m]\}_{m=M-1000}^{M}$ using (7). Figure 2 shows the results for one subject using the three different models. As seen from the figure, the first model performs poorly with the CGM errors and cannot be used to obtain an estimate of the actual blood glucose concentration when compared to the second and third model. The second and third model perform similarly. The chosen covariance functions for the second and third models give the possibility to produce highly correlated time series which are suitable for biases and drifts. It is also seen from the figure that the third model performs slightly better on the first day than the second model while the second model perform slightly better on the second day than the third model.

Additionally, a fit is computed between each sample from $\{\hat{\mathsf{x}}_g^{1:N}[m]\}_{m=M-1000}^{M}$ and the true BG concentration $\mathsf{x}_g^{1:N}$ as following

$$\text{fit}[m] = 1 - \frac{\sqrt{\left(\mathsf{x}_g^{1:N} - \hat{\mathsf{x}}_g^{1:N}[m]\right)^{\mathrm{T}}\left(\mathsf{x}_g^{1:N} - \hat{\mathsf{x}}_g^{1:N}[m]\right)}}{\sqrt{\left(\mathsf{x}_g^{1:N} - \frac{1}{N}\mathbf{1}^{\mathrm{T}}\mathsf{x}_g^{1:N}\right)^{\mathrm{T}}\left(\mathsf{x}_g^{1:N} - \frac{1}{N}\mathbf{1}^{\mathrm{T}}\mathsf{x}_g^{1:N}\right)}}. \tag{12}$$

The mean and standard deviation for the fits over all $m \in \{M - 1000, \ldots, M\}$ are then computed in Table III and reported as a percentage for each model from Table I. It is seen from Table III that the first model performs poorly in general when compared with the other models. It also exhibits a higher uncertainty in the fits (std fits) when compared with the second and the third model. This can also be seen from the subject in Figure 2. The second and third model appear to perform relatively similar. It is seen also that the uncertainty of the fits for the second and third model is much lower than the first model. To asses the precision of the fitted parameters, the dispersion of the posterior is measured by the Quartile Coefficient of Dispersion (QCD) $QCD = \frac{Q_3 - Q_1}{Q_3 + Q_1}$ with Q_1 and Q_3 being the first and the third quantile respectively. The QCD is computed for the posterior of each parameter using the last 1000 samples and the results are reported in Table IV. The reported numbers shows that the parameters $\theta_g, \theta_v, \sigma_c$ were estimated to a better precision when compared to σ_1 and σ_2. This is because for subjects who almost never experienced low BG levels in the simulation, σ_2 was estimated much better than σ_1 since most the time their BG levels were far from 4.2 $[\mathrm{mmol/l}]$ which is the threshold in (8). On the other hand, σ_1 was estimated better for subjects who has lower BG levels for most of the time. Moreover, since more subjects have higher BG levels, the reported QCD values for σ_2 are better than σ_1.

Model	mean fit	std fit
Model 1	72%	14.3%
Model 2	92.5%	5.03%
Model 3	94.2%	1.61%

TABLE III

Mean and standard deviation of fits

Model	θ_g	θ_v	σ_c	σ_1	σ_2
Model 1	0.21, 0.18	0.18, 0.184, 0.23	0.094	0.42	0.31
Model 2	0.11, 0.16	0.112, 0.06	0.064	0.412	0.29
Model 3	0.13, 0.21	0.162, 0.08	0.044	0.425	0.33

TABLE IV

QCD values for the posterior of the parameters. Note that the number of reported QCD values for θ_g and θ_v is based on their dimension.

VIII. Conclusion and Future Work

The suggestion of using TGP in this paper with the presented smoothing strategy has been shown to be able to model correlated and time dependent CGM errors with only one CGM device and SMBG measurements. The TGP models can handle varying parameters for both multiplicative and additive measurement errors on CGM devices. Moreover, the fact that the models and the strategy can be applied with one CGM device and SMBG measurements only make them suitable for subject-specific modeling. For future work, one can investigate different model choices. Additionally, one can use the proposed strategy with the suggested models with real CGM patient data accompanied with detailed BG concentration data sampled at a rate similar to the real CGM device for conformation. Finally, an investigation for improving the smoothing strategy or proposing an alternative one can be carried out.

References

[1] S. Clarke and J. Foster, "A history of blood glucose meters and their role in self-monitoring of diabetes mellitus," *British journal of biomedical science*, vol. 69, no. 2, pp. 83–93, 2012.

[2] B. Kovatchev and C. Cobelli, "Glucose variability: timing, risk analysis, and relationship to hypoglycemia in diabetes," *Diabetes Care*, vol. 39, no. 4, pp. 502–510, 2016.

[3] B. P. Kovatchev, S. D. Patek, E. A. Ortiz, and M. D. Breton, "Assessing sensor accuracy for non-adjunct use of continuous glucose monitoring," *Diabetes technology & therapeutics*, vol. 17, no. 3, pp. 177–186, 2015.

[4] G. Acciaroli, M. Vettoretti, A. Facchinetti, and G. Sparacino, "Chapter 9 - calibration of cgm systems," in *Glucose Monitoring Devices*, C. Fabris and B. Kovatchev, Eds. Academic Press, 2020, pp. 173–201.

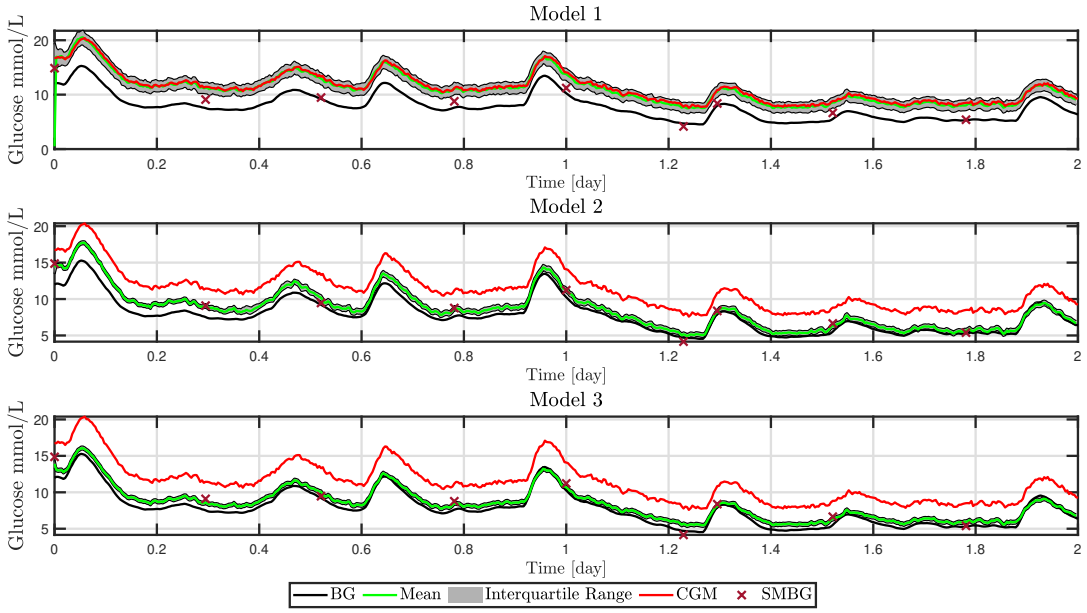

Fig. 2. Results of the smoothing strategy for one subject using the last 1000 samples with the three different Models from Table I

[5] L. Biagi, A. Hirata Bertachi, I. Conget, C. Quirós, M. Giménez, F. J. Ampudia-Blasco, P. Rossetti, J. Bondia, and J. Vehí, "Extensive assessment of blood glucose monitoring during postprandial period and its impact on closed-loop performance," *Journal of diabetes science and technology*, vol. 11, no. 6, pp. 1089–1095, 2017.

[6] C. Boettcher *et al.*, "Accuracy of blood glucose meters for self-monitoring affects glucose control and hypoglycemia rate in children and adolescents with type 1 diabetes," *Diabetes technology & therapeutics*, vol. 17, no. 4, pp. 275–282, 2015.

[7] M. Breton and B. Kovatchev, "Analysis, modeling, and simulation of the accuracy of continuous glucose sensors," *Journal of diabetes science and technology*, vol. 2, no. 5, pp. 853–862, 2008.

[8] D. Lunn, C. Wei, and R. Hovorka, "Fitting dynamic models with forcing functions: application to continuous glucose monitoring in insulin therapy," *Statistics in medicine*, vol. 30, no. 18, pp. 2234–2250, 2011.

[9] A. Facchinetti, S. Del Favero, G. Sparacino, J. R. Castle, W. K. Ward, and C. Cobelli, "Modeling the glucose sensor error," *IEEE Transactions on Biomedical Engineering*, vol. 61, no. 3, pp. 620–629, 2013.

[10] A. Facchinetti, S. Del Favero, G. Sparacino, and C. Cobelli, "Model of glucose sensor error components: identification and assessment for new dexcom g4 generation devices," *Medical & biological engineering & computing*, vol. 53, no. 12, pp. 1259–1269, 2015.

[11] M. Vettoretti, A. Facchinetti, G. Sparacino, and C. Cobelli, "A model of self-monitoring blood glucose measurement error," *Journal of diabetes science and technology*, vol. 11, no. 4, pp. 724–735, 2017.

[12] M. Vettoretti, C. Battocchio, G. Sparacino, and A. Facchinetti, "Development of an error model for a factory-calibrated continuous glucose monitoring sensor with 10-day lifetime," *Sensors*, vol. 19, no. 23, p. 5320, 2019.

[13] E. J. Knobbe and B. Buckingham, "The extended kalman filter for continuous glucose monitoring," *Diabetes technology & therapeutics*, vol. 7, no. 1, pp. 15–27, 2005.

[14] M. Kuure-Kinsey, C. C. Palerm, and B. W. Bequette, "A dual-rate kalman filter for continuous glucose monitoring," in *2006 International Conference of the IEEE Engineering in Medicine and Biology Society*. IEEE, 2006, pp. 63–66.

[15] A. Facchinetti, G. Sparacino, and C. Cobelli, "Enhanced accuracy of continuous glucose monitoring by online extended kalman filtering," *Diabetes technology & therapeutics*, vol. 12, no. 5, pp. 353–363, 2010.

[16] J. C. Boyd and D. E. Bruns, "Quality specifications for glucose meters: assessment by simulation modeling of errors in insulin dose," *Clinical Chemistry*, vol. 47, no. 2, pp. 209–214, 2001.

[17] N. S. Virdi and J. J. Mahoney, "Importance of blood glucose meter and carbohydrate estimation accuracy," *Journal of diabetes science and technology*, vol. 6, no. 4, pp. 921–926, 2012.

[18] M. D. Breton and B. P. Kovatchev, "Impact of blood glucose self-monitoring errors on glucose variability, risk for hypoglycemia, and average glucose control in type 1 diabetes: an in silico study," *Journal of Diabetes Science and Technology*, vol. 4, no. 3, pp. 562–570, 2010.

[19] *In vitro diagnostic test systems: requirements for blood-glucose monitoring systems for self-testing in managing diabetes mellitus*. International Organization for Standardization, 2003.

[20] C. E. Rasmussen, "Gaussian processes in machine learning," in *Summer school on machine learning*. Springer, 2003, pp. 63–71.

[21] J. Hartikainen and S. Särkkä, "Kalman filtering and smoothing solutions to temporal gaussian process regression models," in *2010 IEEE international workshop on machine learning for signal processing*. IEEE, 2010, pp. 379–384.

[22] S. Sarkka, A. Solin, and J. Hartikainen, "Spatiotemporal learning via infinite-dimensional bayesian filtering and smoothing: A look at gaussian process regression through kalman filtering," *IEEE Signal Processing Magazine*, vol. 30, no. 4, pp. 51–61, 2013.

[23] S. Särkkä and R. Piché, "On convergence and accuracy of state-space approximations of squared exponential covariance functions," in *2014 IEEE International Workshop on Machine Learning for Signal Processing (MLSP)*. IEEE, 2014, pp. 1–6.

[24] L. Biagi, C. M. Ramkissoon, A. Facchinetti, Y. Leal, and J. Vehi, "Modeling the error of the medtronic paradigm veo enlite glucose sensor," *Sensors*, vol. 17, no. 6, p. 1361, 2017.

[25] F. Lindsten, M. I. Jordan, and T. B. Schon, "Particle gibbs with ancestor sampling," *Journal of Machine Learning Research*, vol. 15, pp. 2145–2184, 2014.

[26] S. Chib and E. Greenberg, "Understanding the metropolis-hastings algorithm," *The american statistician*, vol. 49, no. 4, pp. 327–335, 1995.

[27] D. Spiegelhalter, A. Thomas, N. Best, and W. Gilks, "Bugs 0.5: Bayesian inference using gibbs sampling manual (version ii)," *MRC Biostatistics Unit, Institute of Public Health, Cambridge, UK*, pp. 1–59, 1996.

[28] M. Al Ahdab, J. Leth, T. Knudsen, P. Vestergaard, and H. G. Clausen, "Glucose-insulin mathematical model for the combined effect of medications and life style of type 2 diabetic patients," *Biochemical Engineering Journal*, vol. 176, p. 108170, 2021.

[29] R. S. Parker, F. J. Doyle III, J. H. Ward, and N. A. Peppas, "Robust $\mathcal{H}_\infty$ glucose control in diabetes using a physiological model," *AIChE Journal*, vol. 46, no. 12, pp. 2537–2549, 2000.